Published in final edited form as:
Immunity. 2011 November 23; 35(5): 780–791. doi:10.1016/j.immuni.2011.08.013.

Notch2 receptor signaling controls functional differentiation of dendritic cells in the spleen and intestine

Kanako L. Lewis[1], **Michele L. Caton**[1], **Milena Bogunovic**[2], **Melanie Greter**[2], **Lucja T. Grajkowska**[1], **Dennis Ng**[3], **Apostolos Klinakis**[4], **Israel F. Charo**[5], **Steffen Jung**[6], **Jennifer L. Gommerman**[3], **Ivaylo I. Ivanov**[1], **Kang Liu**[1], **Miriam Merad**[2], and **Boris Reizis**[1]

[1]Department of Microbiology and Immunology, Columbia University Medical Center, New York, NY 10032, USA

[2]Department of Gene and Cell Medicine, Mount Sinai School of Medicine, New York, NY 10029, USA

[3]Department of Immunology, University of Toronto, Toronto, Ontario M5S 1A8, Canada

[4]Biomedical Research Foundation, Academy of Athens, Athens 11527, Greece

[5]Gladstone Institute of Cardiovascular Disease, University of California, San Francisco, CA 94158, USA

[6]Department of Immunology, The Weizmann Institute of Science, Rehovot, 76100, Israel

Summary

Dendritic cells (DCs) in tissues and lymphoid organs comprise distinct functional subsets that differentiate in situ from circulating progenitors. Tissue-specific signals that regulate DC subset differentiation are poorly understood. We report that DC-specific deletion of the Notch2 receptor caused a reduction of DC populations in the spleen. Within the splenic $CD11b^+$ DC subset, Notch signaling blockade ablated a distinct population marked by high expression of the adhesion molecule Esam. The Notch-dependent $Esam^{hi}$ DC subset required lymphotoxin beta receptor signaling, proliferated in situ and facilitated $CD4^+$ T cell priming. The Notch-independent $Esam^{lo}$ DCs expressed monocyte-related genes and showed superior cytokine responses. In addition, Notch2 deletion led to the loss of $CD11b^+$ $CD103^+$ DCs in the intestinal lamina propria and to a corresponding decrease of IL-17-producing $CD4^+$ T cells in the intestine. Thus, Notch2 is a common differentiation signal for T cell-priming $CD11b^+$ DC subsets in the spleen and intestine.

Introduction

Dendritic cells (DCs) represent the primary antigen (Ag)-presenting cell population in the immune system. They can detect pathogens through pattern recognition receptors such as Toll-like receptors (TLRs), migrate into the T cell areas of lymphoid organs, secrete immunostimulatory cytokines such as interleukin-12 (IL-12), and present pathogen-derived

*Correspondence: B.R. (bvr2101@columbia.edu).

Accession numbers. The microarray data are available in the Gene Expression Omnibus (GEO) database (http://www.ncbi.nlm.nih.gov/gds) under the accession number GSE31551.

peptides to naïve T cells (Steinman and Idoyaga, 2010). To initiate appropriate immune responses to different pathogen types, DCs comprise distinct functional subsets including interferon-producing plasmacytoid DCs (pDCs) and two main subsets of classical DCs. The CD8α-expressing $CD8^+$ $CD11b^-$ DCs in lymphoid organs and their $CD103^+$ $CD11b^-$ counterparts in tissues mediate efficient cross-presentation to cytotoxic T cells (Shortman and Heath, 2010). The CD8α-negative $CD8^-$ $CD11b^+$ subset is preferentially involved in MHC class II (MHC II)-restricted Ag presentation to $CD4^+$ helper T cells (Dudziak et al., 2007). In the spleen, $CD11b^+$ DCs are preferentially localized to the marginal zone (MZ), a unique structure that filters the incoming blood (Mebius and Kraal, 2005). In the intestinal lamina propria (LP), the $CD11b^+$ DC population is comprised of two distinct subsets. The $CD11b^+$ $CD103^+$ subset is thought to mediate Ag capture and transport to mesenteric lymph node (LN). Recently, it was shown to be particularly efficient for the induction of interleukin 17 (IL-17)-secreting helper T cells (Th17) in vitro (Denning et al., 2011), although its role in T cell differentiation in vivo remains unclear. Conversely, the $CD11b^+$ $CD103^-$ population does not migrate to LN, is capable of high-level cytokine secretion and appears closely related to macrophages (Bogunovic et al., 2009; Schulz et al., 2009; Varol et al., 2009).

Classical DCs along with pDCs, monocytes and macrophages originate from the common macrophage and DC progenitor (MDP) in the bone marrow (BM) (Fogg et al., 2006). Commitment to the DC lineage occurs in the BM at the level of common DC progenitors (CDP) (Naik et al., 2007; Onai et al., 2007), whereas the terminal differentiation of classical DC subsets occurs in the periphery. All DCs in the lymphoid organs and $CD8^+$ or $CD103^+$ DCs in tissues are thought to develop from pre-DC (Ginhoux et al., 2009; Liu et al., 2009), a blood-derived progenitor originally defined in the spleen (Naik et al., 2006). Similarly, the unique $CD11b^+$ $CD103^+$ subset in the intestinal LP is derived from pre-DCs. All pre-DC-derived subsets are low or negative for fractalkine receptor Cx3cr1 and preferentially depend on signaling by Flt3 ligand through its receptor Flt3. On the other hand, $CD11b^+$ DCs in tissues arise from MDP-derived monocytes, express Cx3cr1 and depend on macrophage colony-stimulating factor receptor Csf1r rather than on Flt3 (Bogunovic et al., 2009; Ginhoux et al., 2009; Varol et al., 2009). Thus, the homogeneity and single pre-DC origin of DC subsets in lymphoid organs appears to contrast with the functional heterogeneity and dual origin of DC subsets in tissues such as the intestine. Furthermore, little is known about molecular signals that promote DC fate and impart subset and/or specificity on DC progenitors.

Notch is an evolutionarily conserved signaling pathway that allows cells to adopt cell fates dictated by their microenvironment (Bray, 2006). The interaction of Notch receptor with its ligand on a neighboring cell causes receptor cleavage that releases the intracellular domain of Notch (NICD), which translocates into the nucleus and binds the transcription factor CSL (called RBPJ in the mouse). The resulting NICD-RBPJ complex recruits coactivators of the Mastermind (MAML) family and activates Notch-dependent gene expression programs, including canonical targets such as *Hes1* and *Deltex* (*Dtx1*). Notch signaling is regulated at multiple levels including ligand endocytosis, receptor glycosylation and composition of the transactivation complex. Mammals have five Notch ligands of the Delta-like and Jagged families and four Notch receptors (Notch1–4), of which only Notch1 and Notch2 contain transactivation domains. These two receptors appear to mediate the majority of Notch-dependent developmental processes and their deletion causes embryonic lethality.

Notch signaling plays essential roles in lymphocyte development by inducing progenitor differentiation in unique anatomic locations (Radtke et al., 2010; Yashiro-Ohtani et al., 2010; Yuan et al., 2010). Thus, Delta-like 4 (Dll4) on thymic epithelium drives T cell lineage development through Notch1 on thymic progenitors, whereas Delta-like 1 (Dll1) on

the splenic MZ stroma specifies MZ B cell subset through Notch2. However, the role of Notch in the development of innate immune system remains poorly understood. Notch1 has been implicated in DC differentiation in vitro (Cheng et al., 2003; Zhou et al., 2009), although earlier studies on Notch1 deletion in vivo argue against this notion (Radtke et al., 2000). We have shown previously that DC-specific deletion of RBPJ caused partial reduction of the splenic $CD11b^+$ DCs, which express Notch target *Dtx1* in an RBPJ-dependent manner (Caton et al., 2007). However, major questions remain concerning the Notch receptor involved, the partial nature and functional consequences of the phenotype, and the role of Notch in DC differentiation in tissues.

We now report that the Notch2 receptor controls DC differentiation in the spleen. Among the $CD11b^+$ DCs, Notch2-RBPJ signaling specifies a unique $Cx3cr1^{lo}$ $Esam^{hi}$ DC subset, which was required for efficient T cell priming in the spleen. Moreover, Notch2 was necessary for the development of lamina propria $CD11b^+$ $CD103^+$ DCs, which in turn maintain optimal numbers of Th17 cells. These results establish Notch2 signaling as an essential tissue-specific determinant of DC differentiation in the spleen and intestine. Furthermore, they demonstrate that $CD11b^+$ DCs both in tissues and in lymphoid organs are heterogeneous and include a distinct Notch-dependent subset specialized in T cell priming.

Results

Notch2 controls splenic DC differentiation

To determine the role of individual Notch receptors in DC differentiation, we used *Itgax-cre* (*CD11c-cre*) deleter strain for DC-specific deletion of conditional *Notch1* (Radtke et al., 1999) and *Notch2* (McCright et al., 2006) alleles. As a complementary way to block canonical Notch signaling in DCs, we used *Itgax-cre*-induced expression of dominant-negative human MAML1 (DNMAML1) protein fused to green fluorescent protein (GFP) (Tu et al., 2005). The analysis of GFP fluorescence confirmed DC-specific activation of DN*MAML1* expression in the resulting DC-DN*MAML1* mice (Fig. S1). Indeed, Notch2-dependent MZ B cells showed minimal recombination and were present in normal numbers in mice with *Notch2* deletion (DC-$Notch2^{\Delta}$) or with DN*MAML1* activation (Fig. S1). As shown in Fig. 1A,B, mice with DC-specific deletion of *Notch1* (DC-$Notch1^{\Delta}$) had normal splenic DC populations. This is consistent with normal DC development after *Notch1* deletion in hematopoietic chimeras (Radtke et al., 2000). In contrast, DC-$Notch2^{\Delta}$ and DC-DN*MAML1* mice had reduced fraction and absolute numbers of splenic $CD11c^{hi}$ MHC II^+ classical DCs (Fig. 1A,B). The reduction was specific to cDCs, as pDC populations were normal despite efficient *cre* recombination (Fig. S1).

As with DC-specific *Rbpj* deletion (DC-$Rbpj^{\Delta}$, (Caton et al., 2007)), the $CD8^-$ $CD11b^+$ subset was significantly reduced in the spleens of DC-$Notch2^{\Delta}$ and DC-DN*MAML1* mice (Fig. 1C,D). In addition, the $CD8^+$ DC subset was decreased in DC-$Notch2^{\Delta}$ spleens, whereas a distinct population of $CD8^-$ $CD11b^-$ double-negative cells became apparent within the DC population. A similar albeit less pronounced phenotype was observed in DN*MAML1*-overexpressing DCs, suggesting the involvement of canonical Notch signaling. The $CD8^-$ $CD11b^-$ double-negative DCs arising after *Notch2* deletion included two distinct populations expressing either signal regulatory protein alpha (SIRPα) or CD24, the markers associated with $CD11b^+$ and $CD8^+$ DC lineages, respectively (Naik et al., 2006) (Fig. 1E). Similar populations could be detected among the rare $CD8^-$ $CD11b^-$ DCs in wild-type mice, suggesting that they represent natural immature stages of $CD11b^+$ and $CD8^+$ DC development. Earlier developmental stages such as pre-DCs were unaffected by *Notch2* deletion (Fig. S1), consistent with a late differentiation defect.

In addition to the decrease in number, splenic CD11b$^+$ DCs in DC-*Notch2*$^\Delta$ mice exhibited an abnormal surface phenotype including higher CD11b and lower (albeit heterogeneous) SIRPα expression (Fig. 1F). Splenic CD11b$^+$ DCs express the specific marker Dcir2 (33D1) (Dudziak et al., 2007) and a fraction of them express CD4 (Kamath et al., 2000). As shown in Fig. 1F, the fraction of Dcir2$^+$ and CD4$^+$ cells was profoundly reduced in Notch2-deficient CD11b$^+$ DCs. Altogether, these data demonstrate that *Notch2* deletion impairs the development of CD11b$^+$ and CD8$^+$ splenic DCs, and causes phenotypic abnormality of the residual CD11b$^+$ DC population.

Notch2-RBPJ signaling specifies a distinct population of splenic CD8$^-$ DCs

To explain the partial reduction and abnormal phenotype of CD11b$^+$ DCs in DC-*Notch2*$^\Delta$, DC-DN*MAML1* and DC-*Rbpj*$^\Delta$ mice, we hypothesized that CD11b$^+$ DCs are heterogeneous and include a distinct population eliminated by Notch2-RBPJ blockade. We therefore crossed DC-*Rbpj*$^\Delta$ mice to a *Cx3cr1*-GFP reporter strain, which has been used to resolve DC subsets in the spleen and tissues (Bar-On et al., 2010; Varol et al., 2009). We found that CD11b$^+$ DCs in wild-type spleens included GFP^{hi} and GFP^{lo} populations, whereas in DC-*Rbpj*$^\Delta$ spleens the GFP^{lo} population was missing (Fig. 2A). To identify a positive marker of this Notch-dependent DC population, we performed microarray analysis of total CD11b$^+$ DCs from DC-*Rbpj*$^\Delta$ spleens and focused on genes that encode cell surface markers (data not shown). One prominently reduced gene encoded Esam, an immunoglobulin superfamily adhesion molecule that is expressed on endothelium and regulates neutrophil extravasation (Wegmann et al., 2006). We found that among the splenocytes Esam was abundant in a subset of CD11b$^+$ DCs, low in CD8$^+$ DCs and absent from non-DCs (Fig. S2). The combination of Esam with *Cx3cr1*-GFP defined two distinct populations, Esam^{lo} GFP^{hi} and Esam^{hi} GFP^{lo}, the latter completely absent in DC-*Rbpj*$^\Delta$ splenocytes (Fig. 2B). The RBPJ-dependent Esam^{hi} population was also defined by low expression of Clec12a, a C-type lectin expressed by CD8$^+$ DCs, pDCs and myeloid cells (Lahoud et al., 2009). Staining with Esam, particularly in combination with Clec12a, resolved the two CD11b$^+$ DC populations and allowed their analysis in the absence of *Cx3cr1*-GFP reporter (Fig. 2C). The Esam^{hi} but not Esam^{lo} CD11b$^+$ DCs were nearly absent in all examined Notch mutants including DC-*Rbpj*$^\Delta$, DC-*Notch2*$^\Delta$ and DC-DN*MAML1* (Fig. 2D). In contrast, the low Esam expression on CD8$^+$ DCs was minimally affected by *Notch2* loss (Fig. S2).

To test the effect of Notch overactivation in DCs, we used the *Itgax-cre* strain in conjunction with a Cre-inducible overexpression cassette encoding Notch1 intracellular domain (NICD) (Buonamici et al., 2009). The NICDs of Notch1 and Notch2 are highly homologous (Radtke et al., 2010) and are likely interchangeable in gain-of-function experiments. In the resulting DC-NICD animals, splenic CD11b$^+$ DCs consisted almost exclusively of Esam^{hi} Clec12a$^-$ cells (Fig. 2E). Furthermore, the expression of Esam was increased in all DCs including the CD8$^+$ subset (Fig. 2F), showing that Esam as a faithful readout of Notch activity in DCs. Altogether, these data suggest that splenic CD11b$^+$ DCs contain a distinct Esam^{hi} population that is directly regulated by Notch2-RBPJ signaling.

Genetic and phenotypic analysis of splenic Esam^{hi} DCs

We have tested genetic requirements for the development of Notch-dependent Esam^{hi} CD11b$^+$ DC population. Splenocytes from Flt3-deficient mice showed a modest but significant reduction of Esam^{hi} population (Fig. 3A,B), suggesting that Flt3 signaling contributes to its development or homeostasis. The blockade of lymphotoxin β receptor (LTβR) signaling partially reduces the number of splenic CD11b$^+$ DCs and impairs their in situ proliferation in a cell-intrinsic manner (De Trez et al., 2008; Kabashima et al., 2005). We found that the fraction of Esam^{hi} but not of Esam^{lo} DCs was severely reduced in *Ltbr*$^{-/-}$ mice (Fig. 3A,B). To circumvent the pleiotropic defects of LTβR deficiency, we analyzed

competitive chimeras reconstituted with a mixture of wild-type and LTβR-deficient BM. The fraction of LTβR-deficient donor cells was reduced in Esam^{hi} DC population, suggesting that the phenotype was at least partially cell-intrinsic (Fig. 3C,D). In contrast, mice with DC-specific targeting of *Irf4* (Klein et al., 2006), a transcription factor regulating CD11b^{+} DC development, showed marginal decrease of both Esam^{hi} and Esam^{lo} populations (Fig. 3B and data not shown). Thus, Esam^{hi} CD11b^{+} DCs are genetically distinct from Esam^{lo} DCs and specifically depend on Notch2-RBPJ and LTβR signaling, and to a lesser extent on Flt3 signaling.

Cell surface staining of CD11b^{+} DCs showed that the Esam^{hi} Cx3cr1-GFP^{lo} population was uniformly positive for CD4 and Dcir2 (Fig. 4A), in agreement with the preferential loss of CD4^{+} and Dcir2^{+} DCs after Notch2 deletion (Fig. 1F). Conversely, Esam^{lo} Cx3cr1-GFP^{hi} cells were heterogeneous for CD4 and Dcir2 and high for CD11b and Clec12a. Esam^{lo} cells expressed high amounts of Flt3 and LTβR, despite their independence of these receptors (Fig 4A,B and Fig. S3). Cytospin preparations of sorted Esam^{hi} DCs revealed irregular nuclei and thin cytoplasmic veils, whereas Esam^{lo} DCs showed typical mononuclear morphology (Fig 4C). Notably, Esam^{lo} DCs appeared distinct from splenic macrophages (Fig 4C) or intestinal CD11b^{+} CD103$^{−}$ DCs (Bogunovic et al., 2009), as they did not contain prominent cytoplasmic vesicles. After in vivo pulse with nucleoside analogue 5-bromo-2′-deoxyuridine (BrdU), Esam^{hi} CD11b^{+} DC incorporated more BrdU than Esam^{lo} DC (Fig. 4D), revealing a faster turnover. Although the contribution of progenitors cannot be ruled out, the short BrdU pulse revealed more proliferating cells among Esam^{hi} DCs (Fig. 4E). Altogether, the Esam^{hi} subset of CD11b^{+} DCs appears distinct in its higher turnover rate and dependence on Notch2 and LTβR signaling.

Gene expression profiles of splenic CD11b^{+} DC populations

To confirm genetic differences between the two subsets of CD11b^{+} DCs, we compared genome-wide expression profiles of wild-type Esam^{hi} and Esam^{lo} CD11b^{+} DC populations, along with CD11b^{+} DCs from DC-*Rbpj*$^{\Delta}$ mice. No major differences in the expression of Notch2 or other pathway components were found by microarray or quantitative polymerase chain reaction (PCR) (qPCR, Fig. S3), suggesting control by other factors such as ligand availability. Clustering analysis confirmed that RBPJ-deficient DCs were very similar to the Esam^{lo} subset (Fig 5A), as suggested by surface phenotype (Fig. 2). Pairwise comparison of Esam^{hi} and Esam^{lo} populations (Fig. 5B and Table S1) showed the expected differential expression of *Esam* and *Clec12a*. One of the most differentially expressed genes was *Gpr4*, which encodes a G protein-coupled receptor and is preferentially expressed in CD11c^{hi} cDCs as revealed by a *Gpr4* locus-driven transgenic GFP reporter (Fig. S3). This reporter confirmed the expression of *Gpr4* in Esam^{hi} but not Esam^{lo} DCs (Fig. S3). Finally, Esam^{hi} DCs showed lower expression of cell cycle inhibitor Cdkn1a (p21), in accordance with their higher proliferation rate.

Next, the Immgen database (Heng and Painter, 2008) was used to derive expression signatures of splenic CD11b^{+} CD4^{+} and CD11b$^{−}$ CD8^{+} DCs and of blood Ly6C^{+} MHC II^{+} monocytes (Table S2). We then examined the distribution of these signature gene sets among Esam^{hi} and Esam^{lo} CD11b^{+} DC populations. As shown in Fig. 5C, genes characteristic of all DCs were equally expressed by both populations, confirming that they represent bona fide DCs. In contrast, CD11b^{+} DC-specific genes including the Notch target *Dtx1* were preferentially expressed in the Esam^{hi} subset. Conversely, monocyte-specific genes were preferentially expressed in Esam^{lo} cells, including such canonical myeloid genes as *Ly6c*, cytokine (*Csf1r*, *Csf3r*) and chemokine (*Ccr2*) receptors and lysozyme (*Lyz1*, *Lyz2*). Notably, the expression of myeloid genes such as colony stimulating factor (CSF) receptors in Esam^{lo} DCs appear significantly lower than in macrophages (Fig. S3). Thus, the

Esam^{hi} population features the unique expression profile of CD11b^{+} cDCs, whereas Esam^{lo} population appears closer to but distinct from monocytes or macrophages.

Using red fluorescent protein (RFP) reporter driven by *Ccr2* locus (Saederup et al., 2010), we found that Esam^{hi} DCs were the only splenic DC population with low RFP expression, while Esam^{lo} DCs and the majority of CD8^{+} DCs were *Ccr2*-RFP^{hi}. To confirm the differential relationship of Esam^{hi} and Esam^{lo} DCs to myeloid cells, we used lineage tracing with a myeloid-specific *Lyz2-cre* (also known as *LysM-cre*) deleter strain (Jakubzick et al., 2008; Liu et al., 2009). In *Lyz2-cre* mice crossed to a *cre*-inducible yellow fluorescent protein (YFP) reporter, splenic Esam^{hi} DCs as well as CD8^{+} DCs harbored only a small (5–7%) fraction of recombined YFP^{+} cells (Fig. 5E). In contrast, the Esam^{lo} DCs showed substantial recombination (~30%) that was nevertheless lower than in monocytes and macrophages (~45%). These data show that the Esam^{hi} DCs are uniquely low for *Ccr2*, have no developmental history of *Lyz2* expression and therefore are not derived from the Esam^{lo} population or from monocytes.

The differences in signaling requirements, gene expression profile and *Lyz2* expression history suggest that the Esam^{hi} and Esam^{lo} population may arise from different precursors. Indeed, adoptively transferred *Cx3cr1*-GFP^{+} MDP gave rise to both GFP^{hi} and GFP^{lo} splenic CD11b^{+} DC populations, whereas CDP gave rise almost exclusively to GFP^{lo} CD11b^{+} DCs corresponding to the Esam^{hi} subset (Fig. S3). These data suggest that the GFP^{lo} Esam^{hi} subset represents the canonical CDP-derived splenic DC population; conversely, GFP^{hi} DCs likely arise from different myeloid progenitors.

Functional analysis of splenic CD11b^{+} DC populations

The Esam^{lo} DC subset showed preferential expression of multiple genes associated with TLR-mediated pathogen sensing, including several TLRs, MyD88, CD14 and CD36 (Table S1 and Fig. 6A). The expression of these genes in Esam^{lo} DCs was nevertheless lower than in macrophages (Fig. 6B). We therefore tested the ability of CD11b^{+} DC subsets to produce cytokines in response to TLR ligands. Esam^{lo} DCs efficiently produced tumor necrosis factor alpha (TNF-α) and IL-12 in response to the TLR9 agonist CpG DNA, in contrast to the weak production by Esam^{hi} DCs (Fig. 6C). CD11c^{-} CD11b^{+} monocytes and macrophages produced more TNF-α but less IL-12 than Esam^{lo} DCs, underscoring the distinct functionality of the latter population. A similarly superior cytokine production by Esam^{lo} over Esam^{hi} DCs was observed in response to TLR2 agonist heat-killed *L.monocytogenes* (Fig. 6D) and TLR7 agonist gardiquimod (data not shown). No expression of interferon-β or interleukin-10 by either DC population could be detected under these conditions (data not shown). Furthermore, Esam^{lo} DCs showed stronger TLR-mediated induction of costimulatory molecules than Esam^{hi} DCs (Fig. 6E), suggesting a higher overall sensitivity to TLR ligands.

Both subsets of CD11b^{+} DCs showed efficient phagocytosis of in vivo injected polystyrene beads (Fig. S4). In an in vitro Ag presentation assay, both Esam^{lo} and Esam^{hi} DCs sorted from ovalbumin (OVA)-pulsed mice efficiently primed naïve OVA-specific CD4^{+} OT-II T cells (Fig. S4). Furthermore, splenic DCs from DC-*Rbpj*$^{\Delta}$ mice elicited strong OVA-specific OT-II proliferation in vitro, despite lack of the Esam^{hi} DC subset. These data suggest that Esam^{hi} and Esam^{lo} DCs are equally capable of Ag-specific T cell priming in vitro on a per cell basis. To test the role of Esam^{hi} DCs in T cell priming in vivo, we adoptively transferred carboxyfluorescein diacetate succinimidyl ester (CFSE)-labeled OT-II T cells into DC-*Rbpj*$^{\Delta}$ mice and immunized with OVA. Three days after immunization, OT-II T cells showed extensive proliferation (as measured by CFSE dye dilution) in the spleens of control mice, but only minor proliferation in the spleens of DC-*Rbpj*$^{\Delta}$ mice (Fig. 6F). Because DC-

Rbpj$^{\Delta}$ spleens specifically lack Esam^{hi} DCs, we conclude that this subset is required for optimal T cell priming in the spleen in vivo.

Notch2 is required for the development of intestinal CD11b^{+} CD103^{+} DCs

Given the tissue-specific nature of Notch signaling, we examined the role of Notch2 in DC differentiation outside of the spleen. We found that DC-*Notch2*$^{\Delta}$ mice had normal numbers of CD11b^{+} and CD103^{+} DCs and Langerhans cells in the skin and/or skin-draining LN (Fig. S5). Similarly, CD11b^{+} and CD103^{+} DCs in the lung and liver were unaffected by *Notch2* deletion (Fig. S5). However, analysis of DCs in the intestinal LP revealed selective depletion of the CD11b^{+} CD103^{+} subset (Fig. 7A, B). In contrast, the monocyte-derived CD11b^{+} CD103^{-} population was unaffected, whereas the CD103^{+} population was moderately increased. Similarly, the fraction of CD11b^{+} CD103^{+} DCs migrating from the LP was selectively reduced in the mesenteric LN (Fig. 7C). The LP CD11b^{+} CD103^{+} did not express Esam or Dtx1 and were not reduced in DC-*RBPJ*$^{\Delta}$ or DC-DN*MAML1* mice (data not shown), suggesting that the Notch2 signal is transient or qualitatively different in this subset. However, the expression of the *Gpr4* reporter was detected in CD11b^{+} CD103^{+} but not in CD11b^{+} CD103^{-} DCs (Fig. S3). This selective expression was similar to *Gpr4* expression in Esam^{hi} but not Esam^{lo} splenic DCs, illustrating the similarity between Notch2-dependent DC subsets in the spleen and intestine.

To test the functional consequences of CD11b^{+} CD103^{+} DCs depletion, we examined intestinal T cell populations in DC-*Notch2*$^{\Delta}$ mice. While the fraction of regulatory CD4^{+} T (Treg) cells expressing transcription factor FoxP3 was unchanged, the IL-17-producing Th17 cells were reduced ~50% (Fig. 7D). Similar results were observed in the small intestine (Fig. 7D) and colon (not shown). Thus, Notch2 provides a tissue-specific differentiation signal for the CD11b^{+} CD103^{+} DC population, which in turn support optimal effector T cell differentiation in the intestine.

Discussion

Although Notch signaling has been indirectly implicated in various aspects of DC development or function (Caton et al., 2007; Cheng et al., 2003; Feng et al., 2010; Zhou et al., 2009), the specific Notch receptor involved and DC populations affected were unclear. Here we have demonstrated that Notch2 receptor controls the development of specific DC subsets in the spleen and intestine. In contrast, Notch1 was dispensable for DC development, consistent with previous results of global inducible *Notch1* deletion (Radtke et al., 2000). Similarly, Notch4 deficiency did not affect DC populations (data not shown), establishing Notch2 as a non-redundant Notch receptor regulating the DC lineage development.

Canonical Notch signaling occurs through the NICD-RBPJ-MAML transcriptional activation complex, and *Rbpj* deletion (Han et al., 2002) or DNMAML1-mediated complex disruption (Maillard et al., 2004) recapitulates Notch receptor deletion in lymphocytes. Indeed, CD11b^{+} splenic DCs were equally affected by the loss of Notch2 or RBPJ or by DNMAML expression. However, *Notch2* deletion impaired the development of splenic CD8^{+} DCs and intestinal CD11b^{+} CD103^{+} DCs, whereas *Rbpj* deletion spared both subsets ((Caton et al., 2007) and data not shown). Although Notch2 signaling in these DC subsets may include a non-canonical RBPJ-independent pathway, this discrepancy likely reflects technical aspects of gene targeting in DCs. Because DCs have a rapid turnover and *Itgax-cre* recombination commences after DC commitment, delayed recombination kinetics and/or increased protein perdurance of RBPJ versus Notch2 would mitigate the phenotype. Indeed, continuous global deletion of RBPJ caused apparent loss of CD8^{+} DCs (Feng et al., 2010), suggesting the predominant role of canonical Notch2 signaling in DC development.

Notch signaling can provide the initial commitment signal as well as sustain further differentiation steps and/or homeostasis of a given cell type (Radtke et al., 2010; Yashiro-Ohtani et al., 2010). In splenic DCs, *Notch2* deletion affected both DC subsets and caused accumulation of immature $CD11b^{-}$ $CD8^{-}$ cells. In addition, mature $CD11b^{+}$ DCs demonstrate ongoing Notch signaling activity, as evidenced by RBPJ-dependent expression of *Dtx1* and sensitivity to Notch2-RBPJ loss or DNMAML1 induction. In contrast, $CD8^{+}$ DCs do not express *Dtx1* and are less affected by *Rbpj* deletion or DN*MAML1* induction. Thus, Notch2 signaling appears to initiate and maintain the differentiation of splenic $CD11b^{+}$ DC subset, starting at the common pre-DC stage and thereby promoting $CD8^{+}$ DC development as well. In tissues such as the intestine, Notch signaling in $CD11b^{+}$ $CD103^{+}$ DCs may commence after the pre-DC stage, and would not affect $CD103^{+}$ DCs.

Our data illustrate a tissue-specific role of Notch signaling in DC differentiation in the spleen and intestinal LP, in contrast to its proposed general role in DC development (Cheng et al., 2003; Zhou et al., 2009). Indeed, both tissues are classical sites of Notch activity, which drives the respective differentiation of splenic MZ B cells and of the intestinal epithelium (Wilson and Radtke, 2006). MZ B cell development is mediated solely by Notch ligand Dll1 (Hozumi et al., 2004), whereas the latter involves both Dll1 and Dll4 (Pellegrinet et al., 2011). Because both Dll1 and Dll4 are also expressed in the splenic red pulp and MZ (Tan et al., 2009), these two ligands may redundantly regulate Notch2-mediated DC development both in the spleen and intestine. A notable molecular feature of the splenic MZ is active LTβR signaling, which is required both for MZ formation and MZ B cell maintenance, likely in a cell-extrinsic manner (Mebius and Kraal, 2005). We found that both Notch2 and LTβR signals control the development of $CD11b^{+}$ splenic DCs. The contribution of LTβR was at least in part intrinsic to the hematopoietic compartment, consistent with previous studies on LTβR in DC development (Kabashima et al., 2005) and function (Summers deLuca et al., 2011). Our results establish these two pathways as common regulators of the splenic MZ and of its two major immune constituents, the MZ B cells and $CD11b^{+}$ DCs.

The $CD11b^{+}$ and $CD8^{+}$ DC populations in the lymphoid organs of naive animals were thought to be genetically and functionally homogeneous. However, it has been demonstrated recently that $CD8^{+}$ DCs are comprised of two distinct populations, the *Cx3cr1*-GFP^{-} classical $CD8^{+}$ DCs and *Cx3cr1*-GFP^{hi} cells affiliated with the pDC lineage (Bar-On et al., 2010). Here we combined genetic analysis with the *Cx3cr1*-GFP reporter and surface marker Esam to similarly sub-divide the splenic $CD11b^{+}$ DCs. In particular, we found that Notch or LTβR signaling blockade causes a complete ablation of the $Esam^{hi}$ DC subset, rather than a partial decrease of all splenic $CD11b^{+}$ DCs. The Notch2-dependent $Esam^{hi}$ population exhibited properties of classical DCs, including cytoplasmic “veils” and rapid turnover. Although the $CD4^{+}$ subset of $CD11b^{+}$ DCs was reported to incorporate BrdU at a slower rate (Kamath et al., 2000), Esam is expressed only in a fraction of $CD4^{+}$ DCs and thus provides a more precise subset definition. Furthermore, the higher turnover of RBPJ-deficient $CD11b^{+}$ DCs (Caton et al., 2007) was based on prolonged BrdU pulse that aggregated proliferation with cell death and migration. Most importantly, the higher proliferation rate of $Esam^{hi}$ DCs is consistent with their dependence on Flt3 and LTβR signaling, both of which promote DC proliferation in situ (Kabashima et al., 2005; Waskow et al., 2008).

All blood-derived DCs in lymphoid organs are thought to originate from CDPs in the BM via the committed pre-DCs entering from the blood and differentiating in situ. Indeed, the $Esam^{hi}$ $Cx3cr1^{lo}$ $CD11b^{+}$ splenic DCs apparently arise in this pathway as they can be derived from CDPs and lack developmental history of myeloid-specific *Lyz2* gene expression. In contrast, the $Esam^{lo}$ $Cx3cr1^{hi}$ subset could not be derived from transferred

CDPs and preferentially expressed myeloid genes, although at much lower level than monocytes or macrophages. Because splenic DCs cannot be derived from monocytes (Varol et al., 2007), the Esam^{lo} DCs likely arise from earlier progenitors such as MDPs. Splenic DC development is not dependent on myeloid cytokine receptors Csf1r (Ginhoux et al., 2009) or Csf2r (our unpublished data), consistent with the lower expression of these genes in Esam^{lo} DCs relative to macrophages (Fig. S3). In any case, our results suggest that the spleen is similar to non-lymphoid organs in the dual origin of its resident DCs from the CDPs and from a parallel myelomonocytic pathway.

In the spleen, the absence of Esam^{hi} DCs after DC-specific *Rbpj* deletion impaired CD4^{+} T cell priming. This was not due to higher Ag uptake or presentation capacity of Esam^{hi} DCs on a per cell basis; therefore, Esam^{hi} DCs may be uniquely suited for T cell priming because of their specific localization in the MZ and/or migration properties. In the intestinal LP, the CD11b^{+} CD103^{+} cells represent a unique DC population that migrates to the mesenteric LN in the steady state and upon inflammation, suggesting its likely role in T cell priming (Bogunovic et al., 2009). We found that the loss of this population after DC-specific *Notch2* targeting was associated with a reduced fraction of Th17 T cells, a major effector CD4^{+} T cell population in the intestine. Although this finding remains to be confirmed in mice with pure genetic background and more defined microflora, it is consistent with the recently reported capacity of CD11b^{+} CD103^{+} DCs to induce Th17 cell differentiation in vitro (Denning et al., 2011). Thus, DC-specific Notch2 targeting provided the first insight into the specific function of CD11b^{+} CD103^{+} DC subset in vivo, opening the way for future studies of immune responses and tolerance in the intestine. Collectively, our results establish Notch2 as a common regulator of the two key T cell-priming DC populations in the spleen and the intestine.

Methods

Animals

The *Itgax-cre* hemizygous transgene was used to generate the following experimental animals on C57BL/6 (B6) background unless indicated otherwise: DC-*Rbpj*$^{\Delta}$ (*Rbpj*$^{flox/flox}$), DC-*Notch1*$^{\Delta}$ (*Notch1*$^{flox/flox}$), DC-*Notch2*$^{\Delta}$ (*Notch2*$^{flox/flox}$, mixed B6/129), DC-*Irf4*$^{\Delta}$ (*Irf4*$^{flox/flox}$), DC-DN*MAML1* (*Rosa26*-StopFlox-DN*MAML1*, B6 or B6129F1), DC-NICD (*Eef1a1*-StopFlox-NICD1, mixed B6/129). Where indicated, DC-*Rbpj*$^{\Delta}$ mice carried heterozygous *Cx3cr1*-GFP reporter allele. Because the *Itgax-cre* transgene does not affect DC numbers or phenotype (Caton et al., 2007), Cre-negative littermates were used as controls for the respective *Itgax-cre*$^{+}$ animals. For the analysis of intestinal T cells, co-housed sex-matched littermates were used. Germline null mutants of Flt3 and LTβR on B6 background, as well as competitive chimeras established from LTβR-null BM have been described (Summers deLuca et al., 2011; Waskow et al., 2008). Chimeras were analyzed 11 weeks after reconstitution and the donor- or competitor-derived cells were distinguished by differential CD45 isoform expression. Homo- or heterozygous *Cx3cr1*-GFP and heterozygous *Ccr2*-RFP reporter mice were on the B6 background. The *Lyz2-cre* lineage tracing was performed as described (Jakubzick et al., 2008), and utilized mice hemizygous for *Lyz2*-cre and heterozygous for *Rosa26*-StopFlox-EYFP. All animal studies were performed according to the investigator's protocol approved by the Institutional Animal Care and Use Committee of Columbia University.

Cell analysis

Cells were isolated *ex vivo* from lymphoid organs and stained for cell surface markers as described (Caton et al., 2007; Liu et al., 2009). The antibodies used for staining are listed in Table S3. The isolation and analysis of DCs from the intestinal LP and other tissues was

done as in (Bogunovic et al., 2009; Ginhoux et al., 2009). The isolation and analysis of intestinal T cells was done as described (Ivanov et al., 2006). Fluorochrome- or biotin-conjugated antibodies were from eBiosciences or BD Biosciences. Biotinylated anti-Clec12a was kindly provided by Dr. M. Lahoud, at the Walter and Eliza Hall Institute. The samples were acquired on a LSR II flow cytometer or sorted on FACSAria flow sorter (BD Immunocytometry Systems), and analyzed using FlowJo software (Treestar Inc.). Cytospin preparations were done on Cytospin 3 centrifuge (Thermo Shandon) and stained by Giemsa stain.

For BrdU incorporation, *Cx3cr1*-GFP reporter mice were either injected i.p. with 1.5 mg BrdU and analyzed 2 hr later, or injected with 1.5 mg BrdU for two consecutive days and analyzed 48 hr after the first injection. BrdU staining was performed using APC BrdU Flow Kit (BD Biosciences), and combined with DAPI staining for 2 hr pulse. To measure cytokine production, splenocytes from *Cx3cr1*-GFP mice were depleted of lymphoid and erythroid cells by negative selection on MACS columns (Miltenyi). The DC-enriched flow-through fraction was incubated in serum-containing medium at 37°C with 100 nM CpG-B oligonucleotides (ODN1826) or 10^8 heat-killed *L.monocytogenes* (Invivogen). After 2 hours, Brefeldin A (10 μg/ml) was added and the cells were incubated for an additional 4 hrs. Cells were stained for surface markers, fixed, permeabilized and stained with APC-conjugated antibodies to IL-12 or TNF-α (BD Biosciences) according to the manufacturer's instructions.

Gene expression analysis

For microarray analysis, spleens from *Cx3cr1*-GFP$^+$ DC-*Rbpj*$^\Delta$ mice or Cre-negative littermate controls were isolated and depleted of lymphoid and erythroid cells by negative selection on MACS columns. Total CD11c^{hi} CD11b$^+$ DCs from DC-*Rbpj*$^\Delta$ spleens (uniformly Esam^{lo} GFP^{hi}, see Fig. 2) or Esam^{lo} GFP^{hi} and Esam^{hi} GFP^{lo} subsets thereof from control mice were sorted and total RNA was isolated using RNeasy columns (Qiagen). Precipitated RNA was reverse-transcribed, labeled, and hybridized to GeneChip Mouse Gene 1.0 ST Array (Affymetrix) according to the manufacturer's instructions. RMA-normalized gene expression values were analyzed using NIA Array software (Sharov et al., 2005). The signatures of normal DC populations were derived by clustering analysis of Immgen subsets DC.4+.Sp, DC.8+.Sp and Mo.6c+II+.Bl (Heng and Painter, 2008). Real-time qPCR was performed as described (Caton et al., 2007).

T cell proliferation assay

Splenic and LN CD4$^+$ T cells from OVA-specific OT-II transgenic mice (Barnden et al., 1998) were enriched by negative selection using MACS columns, labeled with CFSE and injected intravenously (i.v.) (2×10^6 per animal) into DC-*Rbpj*$^\Delta$ or control mice. After 24 hr recipient mice received 10 mg OVA (Sigma) i.v. and were analyzed 72 hr later. Transferred T cells were identified as CD4$^+$ TCR Vα2$^+$ TCR Vβ5$^+$.

Statistical analysis

Statistical significance was estimated using unpaired, two-tailed Student's *t*-test.

Supplementary Material

Refer to Web version on PubMed Central for supplementary material.

Acknowledgments

We thank U. Klein, A. Efstratiadis, F. Radtke, T. Gridley and W. Pear for mouse strains, A. Capobianco, D. Lin and A. Ferrante for animal donations, M. Lahoud for antibodies and J. Ericson for Immgen data. Supported by the American Asthma Foundation (B.R.), NIH grants AI072571 (B.R.) and DK085329 (I.I.I.), NIH training grants AI007161 (K.L.L.) and HD055165 (M.L.C.), and CIHR/IRSC award MOP #67157 (J.L.G.).

References

Bar-On L, Birnberg T, Lewis KL, Edelson BT, Bruder D, Hildner K, Buer J, Murphy KM, Reizis B, Jung S. CX3CR1+ CD8alpha+ dendritic cells are a steady-state population related to plasmacytoid dendritic cells. Proc Natl Acad Sci U S A. 2010; 107:14745–14750. [PubMed: 20679228]

Barnden MJ, Allison J, Heath WR, Carbone FR. Defective TCR expression in transgenic mice constructed using cDNA-based alpha- and beta-chain genes under the control of heterologous regulatory elements. Immunol Cell Biol. 1998; 76:34–40. [PubMed: 9553774]

Bogunovic M, Ginhoux F, Helft J, Shang L, Hashimoto D, Greter M, Liu K, Jakubzick C, Ingersoll MA, Leboeuf M, et al. Origin of the lamina propria dendritic cell network. Immunity. 2009; 31:513–525. [PubMed: 19733489]

Bray SJ. Notch signalling: a simple pathway becomes complex. Nat Rev Mol Cell Biol. 2006; 7:678–689. [PubMed: 16921404]

Buonamici S, Trimarchi T, Ruocco MG, Reavie L, Cathelin S, Mar BG, Klinakis A, Lukyanov Y, Tseng JC, Sen F, et al. CCR7 signalling as an essential regulator of CNS infiltration in T-cell leukaemia. Nature. 2009; 459:1000–1004. [PubMed: 19536265]

Caton ML, Smith-Raska MR, Reizis B. Notch-RBP-J signaling controls the homeostasis of CD8- dendritic cells in the spleen. J Exp Med. 2007; 204:1653–1664. [PubMed: 17591855]

Cheng P, Nefedova Y, Miele L, Osborne BA, Gabrilovich D. Notch signaling is necessary but not sufficient for differentiation of dendritic cells. Blood. 2003; 102:3980–3988. [PubMed: 12907456]

De Trez C, Schneider K, Potter K, Droin N, Fulton J, Norris PS, Ha SW, Fu YX, Murphy T, Murphy KM, et al. The inhibitory HVEM-BTLA pathway counter regulates lymphotoxin receptor signaling to achieve homeostasis of dendritic cells. J Immunol. 2008; 180:238–248. [PubMed: 18097025]

Denning TL, Norris BA, Medina-Contreras O, Manicassamy S, Geem D, Madan R, Karp CL, Pulendran B. Functional Specializations of Intestinal Dendritic Cell and Macrophage Subsets That Control Th17 and Regulatory T Cell Responses Are Dependent on the T Cell/APC Ratio, Source of Mouse Strain, and Regional Localization. J Immunol. 2011; 187:733–747. [PubMed: 21666057]

Dudziak D, Kamphorst AO, Heidkamp GF, Buchholz VR, Trumpfheller C, Yamazaki S, Cheong C, Liu K, Lee HW, Park CG, et al. Differential antigen processing by dendritic cell subsets in vivo. Science. 2007; 315:107–111. [PubMed: 17204652]

Feng F, Wang YC, Hu XB, Liu XW, Ji G, Chen YR, Wang L, He F, Dou GR, Liang L, et al. The transcription factor RBP-J-mediated signaling is essential for dendritic cells to evoke efficient anti-tumor immune responses in mice. Mol Cancer. 2010; 9:90. [PubMed: 20420708]

Fogg DK, Sibon C, Miled C, Jung S, Aucouturier P, Littman DR, Cumano A, Geissmann F. A clonogenic bone marrow progenitor specific for macrophages and dendritic cells. Science. 2006; 311:83–87. [PubMed: 16322423]

Ginhoux F, Liu K, Helft J, Bogunovic M, Greter M, Hashimoto D, Price J, Yin N, Bromberg J, Lira SA, et al. The origin and development of nonlymphoid tissue CD103+ DCs. J Exp Med. 2009; 206:3115–3130. [PubMed: 20008528]

Han H, Tanigaki K, Yamamoto N, Kuroda K, Yoshimoto M, Nakahata T, Ikuta K, Honjo T. Inducible gene knockout of transcription factor recombination signal binding protein-J reveals its essential role in T versus B lineage decision. Int Immunol. 2002; 14:637–645. [PubMed: 12039915]

Heng TS, Painter MW. The Immunological Genome Project: networks of gene expression in immune cells. Nat Immunol. 2008; 9:1091–1094. [PubMed: 18800157]

Hozumi K, Negishi N, Suzuki D, Abe N, Sotomaru Y, Tamaoki N, Mailhos C, Ish-Horowicz D, Habu S, Owen MJ. Delta-like 1 is necessary for the generation of marginal zone B cells but not T cells in vivo. Nat Immunol. 2004; 5:638–644. [PubMed: 15146182]

Ivanov II, McKenzie BS, Zhou L, Tadokoro CE, Lepelley A, Lafaille JJ, Cua DJ, Littman DR. The orphan nuclear receptor RORgammat directs the differentiation program of proinflammatory IL-17+ T helper cells. Cell. 2006; 126:1121–1133. [PubMed: 16990136]

Jakubzick C, Bogunovic M, Bonito AJ, Kuan EL, Merad M, Randolph GJ. Lymph-migrating, tissue-derived dendritic cells are minor constituents within steady-state lymph nodes. J Exp Med. 2008; 205:2839–2850. [PubMed: 18981237]

Kabashima K, Banks TA, Ansel KM, Lu TT, Ware CF, Cyster JG. Intrinsic lymphotoxin-beta receptor requirement for homeostasis of lymphoid tissue dendritic cells. Immunity. 2005; 22:439–450. [PubMed: 15845449]

Kamath AT, Pooley J, O'Keeffe MA, Vremec D, Zhan Y, Lew AM, D'Amico A, Wu L, Tough DF, Shortman K. The development, maturation, and turnover rate of mouse spleen dendritic cell populations. J Immunol. 2000; 165:6762–6770. [PubMed: 11120796]

Klein U, Casola S, Cattoretti G, Shen Q, Lia M, Mo T, Ludwig T, Rajewsky K, Dalla-Favera R. Transcription factor IRF4 controls plasma cell differentiation and class-switch recombination. Nat Immunol. 2006; 7:773–782. [PubMed: 16767092]

Lahoud MH, Proietto AI, Ahmet F, Kitsoulis S, Eidsmo L, Wu L, Sathe P, Pietersz S, Chang HW, Walker ID, et al. The C-type lectin Clec12A present on mouse and human dendritic cells can serve as a target for antigen delivery and enhancement of antibody responses. J Immunol. 2009; 182:7587–7594. [PubMed: 19494282]

Liu K, Victora GD, Schwickert TA, Guermonprez P, Meredith MM, Yao K, Chu FF, Randolph GJ, Rudensky AY, Nussenzweig M. In Vivo Analysis of Dendritic Cell Development and Homeostasis. Science. 2009; 324:392–397. [PubMed: 19286519]

Maillard I, Weng AP, Carpenter AC, Rodriguez CG, Sai H, Xu L, Allman D, Aster JC, Pear WS. Mastermind critically regulates Notch-mediated lymphoid cell fate decisions. Blood. 2004; 104:1696–1702. [PubMed: 15187027]

McCright B, Lozier J, Gridley T. Generation of new Notch2 mutant alleles. Genesis. 2006; 44:29–33. [PubMed: 16397869]

Mebius RE, Kraal G. Structure and function of the spleen. Nat Rev Immunol. 2005; 5:606–616. [PubMed: 16056254]

Naik SH, Metcalf D, van Nieuwenhuijze A, Wicks I, Wu L, O'Keeffe M, Shortman K. Intrasplenic steady-state dendritic cell precursors that are distinct from monocytes. Nat Immunol. 2006; 7:663–671. [PubMed: 16680143]

Naik SH, Sathe P, Park HY, Metcalf D, Proietto AI, Dakic A, Carotta S, O'Keeffe M, Bahlo M, Papenfuss A, et al. Development of plasmacytoid and conventional dendritic cell subtypes from single precursor cells derived in vitro and in vivo. Nat Immunol. 2007; 8:1217–1226. [PubMed: 17922015]

Onai N, Obata-Onai A, Schmid MA, Ohteki T, Jarrossay D, Manz MG. Identification of clonogenic common Flt3+M-CSFR+ plasmacytoid and conventional dendritic cell progenitors in mouse bone marrow. Nat Immunol. 2007; 8:1207–1216. [PubMed: 17922016]

Pellegrinet L, Rodilla V, Liu Z, Chen S, Koch U, Espinosa L, Kaestner KH, Kopan R, Lewis J, Radtke F. Dll1- and dll4-mediated notch signaling are required for homeostasis of intestinal stem cells. Gastroenterology. 2011; 140:1230–1240. e1237. [PubMed: 21238454]

Radtke F, Fasnacht N, Macdonald HR. Notch signaling in the immune system. Immunity. 2010; 32:14–27. [PubMed: 20152168]

Radtke F, Ferrero I, Wilson A, Lees R, Aguet M, MacDonald HR. Notch1 deficiency dissociates the intrathymic development of dendritic cells and T cells. J Exp Med. 2000; 191:1085–1094. [PubMed: 10748227]

Radtke F, Wilson A, Stark G, Bauer M, van Meerwijk J, MacDonald HR, Aguet M. Deficient T cell fate specification in mice with an induced inactivation of Notch1. Immunity. 1999; 10:547–558. [PubMed: 10367900]

Saederup N, Cardona AE, Croft K, Mizutani M, Cotleur AC, Tsou CL, Ransohoff RM, Charo IF. Selective chemokine receptor usage by central nervous system myeloid cells in CCR2-red fluorescent protein knock-in mice. PLoS One. 2010; 5:e13693. [PubMed: 21060874]

Schulz O, Jaensson E, Persson EK, Liu X, Worbs T, Agace WW, Pabst O. Intestinal CD103+, but not CX3CR1+, antigen sampling cells migrate in lymph and serve classical dendritic cell functions. J Exp Med. 2009; 206:3101–3114. [PubMed: 20008524]

Sharov AA, Dudekula DB, Ko MS. A web-based tool for principal component and significance analysis of microarray data. Bioinformatics. 2005; 21:2548–2549. [PubMed: 15734774]

Shortman K, Heath WR. The CD8+ dendritic cell subset. Immunol Rev. 2010; 234:18–31. [PubMed: 20193009]

Steinman RM, Idoyaga J. Features of the dendritic cell lineage. Immunol Rev. 2010; 234:5–17. [PubMed: 20193008]

Summers deLuca L, Ng D, Gao Y, Wortzman ME, Watts TH, Gommerman JL. LTbetaR signaling in dendritic cells induces a type I IFN response that is required for optimal clonal expansion of CD8+ T cells. Proc Natl Acad Sci U S A. 2011; 108:2046–2051. [PubMed: 21245292]

Tan JB, Xu K, Cretegny K, Visan I, Yuan JS, Egan SE, Guidos CJ. Lunatic and manic fringe cooperatively enhance marginal zone B cell precursor competition for delta-like 1 in splenic endothelial niches. Immunity. 2009; 30:254–263. [PubMed: 19217325]

Tu L, Fang TC, Artis D, Shestova O, Pross SE, Maillard I, Pear WS. Notch signaling is an important regulator of type 2 immunity. J Exp Med. 2005; 202:1037–1042. [PubMed: 16230473]

Varol C, Landsman L, Fogg DK, Greenshtein L, Gildor B, Margalit R, Kalchenko V, Geissmann F, Jung S. Monocytes give rise to mucosal, but not splenic, conventional dendritic cells. J Exp Med. 2007; 204:171–180. [PubMed: 17190836]

Varol C, Vallon-Eberhard A, Elinav E, Aychek T, Shapira Y, Luche H, Fehling HJ, Hardt WD, Shakhar G, Jung S. Intestinal lamina propria dendritic cell subsets have different origin and functions. Immunity. 2009; 31:502–512. [PubMed: 19733097]

Waskow C, Liu K, Darrasse-Jeze G, Guermonprez P, Ginhoux F, Merad M, Shengelia T, Yao K, Nussenzweig M. The receptor tyrosine kinase Flt3 is required for dendritic cell development in peripheral lymphoid tissues. Nat Immunol. 2008; 9:676–683. [PubMed: 18469816]

Wegmann F, Petri B, Khandoga AG, Moser C, Khandoga A, Volkery S, Li H, Nasdala I, Brandau O, Fassler R, et al. ESAM supports neutrophil extravasation, activation of Rho, and VEGF-induced vascular permeability. J Exp Med. 2006; 203:1671–1677. [PubMed: 16818677]

Wilson A, Radtke F. Multiple functions of Notch signaling in self-renewing organs and cancer. FEBS Lett. 2006; 580:2860–2868. [PubMed: 16574107]

Yashiro-Ohtani Y, Ohtani T, Pear WS. Notch regulation of early thymocyte development. Semin Immunol. 2010; 22:261–269. [PubMed: 20630772]

Yuan JS, Kousis PC, Suliman S, Visan I, Guidos CJ. Functions of notch signaling in the immune system: consensus and controversies. Annu Rev Immunol. 2010; 28:343–365. [PubMed: 20192807]

Zhou J, Cheng P, Youn JI, Cotter MJ, Gabrilovich DI. Notch and wingless signaling cooperate in regulation of dendritic cell differentiation. Immunity. 2009; 30:845–859. [PubMed: 19523851]

Highlights

- Notch2 controls differentiation of splenic classical DCs
- Notch2 dependence defines a distinct Esam^{hi} population of splenic CD11b^{+} DCs
- The Esam^{hi} CD11b^{+} DCs are required for CD4^{+} T cell priming in the spleen
- Notch2 controls differentiation of CD11b^{+} CD103^{+} DCs in the intestinal lamina propria

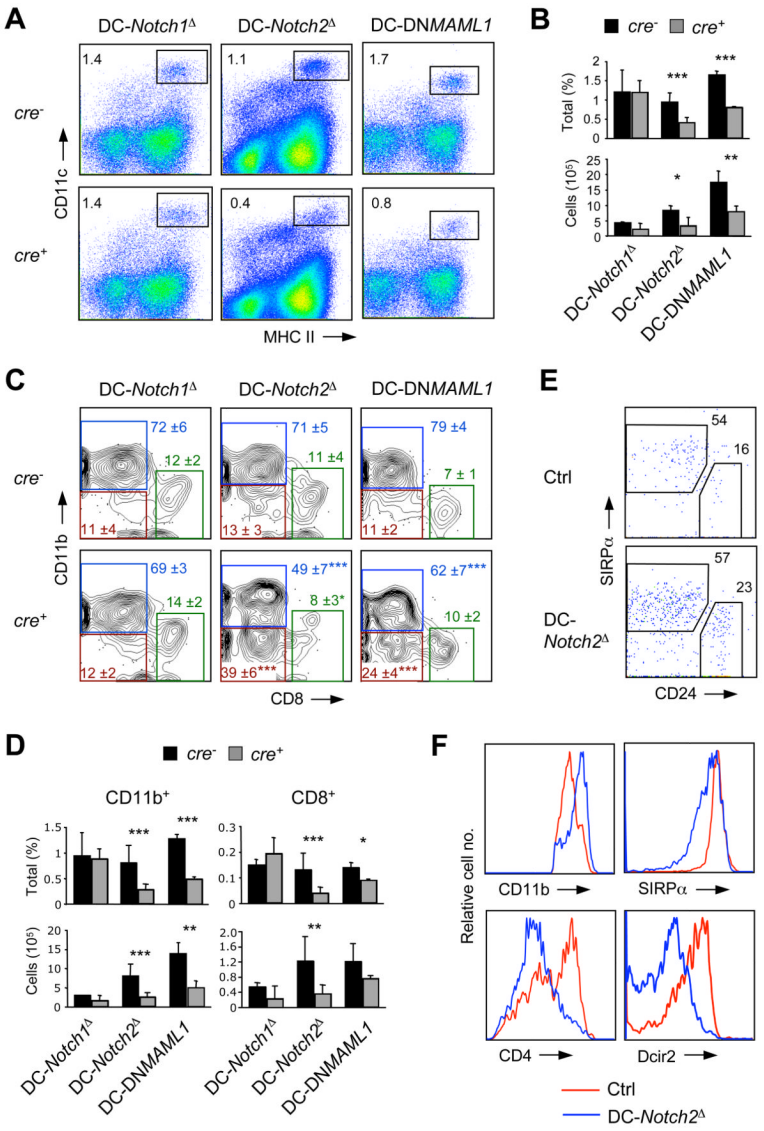

Figure 1. Notch2 signaling regulates splenic DC development

Mice with *Itgax-cre* -mediated deletion of *Notch1* or *Notch2* or DC-specific overexpression of DN*MAML1* were analyzed along with the respective *cre*-negative littermate controls. Statistically significant differences are indicated as follows: ***, P<0.001; **, P<0.01; *, P<0.05.

(A) Representative staining profiles of total splenocytes with the fraction of CD11c^{hi} MHC II^{+} DCs indicated.

(B) The fraction (top) and absolute number (bottom) of splenic DCs (mean ± S.D. of 3–6 animals per group).

(C) Staining profiles of gated CD11c^{hi} MHC II^{+} splenic DCs, with CD11b^{+} (blue), CD8^{+} (green), and double-negative (purple) subsets highlighted. The percentages represent mean ± S.D., n=3–6 for DC-*Notch1*$^{\Delta}$ and DC-DN*MAML1* and 11–12 for DC-*Notch2*$^{\Delta}$.

(D) The percentage among total splenocytes (top) and absolute number (bottom) of CD11b^{+} and CD8^{+} DC subsets (mean ± S.D. of 8–10 animals per group).

(E) The expression of SIRPα and CD24 in gated CD11c^{hi} MHC II^{+} CD11b^{-} CD8^{-} double-negative DCs from conditional *Notch2* (DC-*Notch2*$^{\Delta}$) and littermate control (Ctrl) spleens.

The SIRPα^{+} and CD24^{+} populations indicative of the differentiation towards CD11b^{+} and CD8^{+} DC subsets, respectively, are indicated (representative of 2 animals).
(F) Expression of surface markers in CD11b^{+} DCs from DC-*Notch2*$^{\Delta}$ and control spleens.

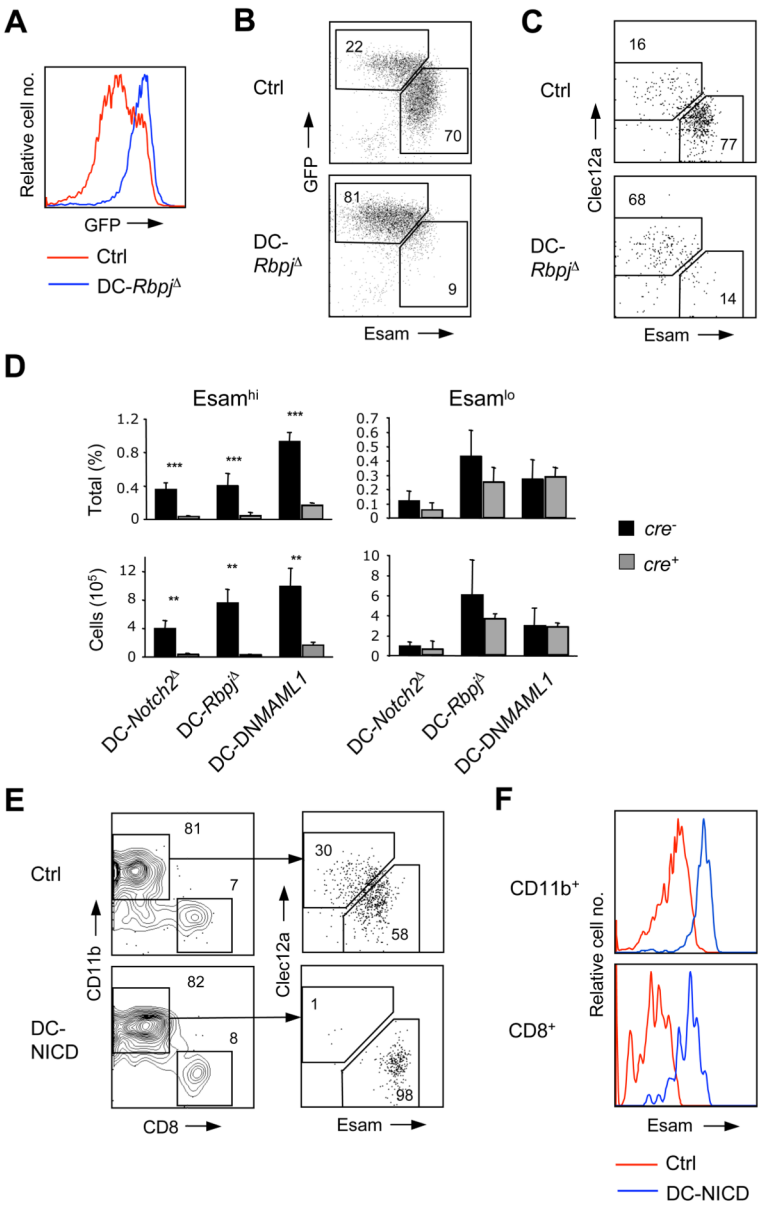

Figure 2. Notch2-RBPJ signaling specifies a distinct population of CD11b$^+$ cDC

(A) The expression of *Cx3cr1*-GFP reporter in CD11b$^+$ splenic DCs from conditional RBPJ-deficient (DC-*Rbpj*$^\Delta$) mice. Shown is the histogram of GFP expression in gated CD11c^{hi} MHC II$^+$ CD11b$^+$ DCs from *Cx3cr1*-GFP$^+$ control (Ctrl) or DC-*Rbpj*$^\Delta$ mice (representative of 4 animals per group).

(B) The expression of Esam vs GFP in gated CD11b$^+$ splenic DCs from *Cx3cr1*-GFP$^+$ control or DC-*Rbpj*$^\Delta$ mice.

(C) The expression of Esam vs Clec12a in gated CD11b$^+$ splenic DCs from DC-*Rbpj*$^\Delta$ or control mice.

(D) The percentage among total splenocytes (top) and absolute number (bottom) of the Esam^{hi} and Esam^{lo} CD11b$^+$ DC subsets in mice with DC-specific targeting of the indicated genes (mean ± S.D. of 3–5 animals). Significance is indicated as in Fig. 1.

(E) Splenic DC populations in mice with DC-specific expression of Notch1 intracellular domain (DC-NICD). Shown are staining profiles of gated splenic CD11c^{hi} MHC II$^+$ DCs

and of their CD11b$^+$ subset from DC-NICD mice or Cre-negative littermate controls (Ctrl). Representative of 8 animals per genotype.
(F) The expression of Esam in splenic CD11b$^+$ and CD8$^+$ DCs from DC-NICD and control mice.

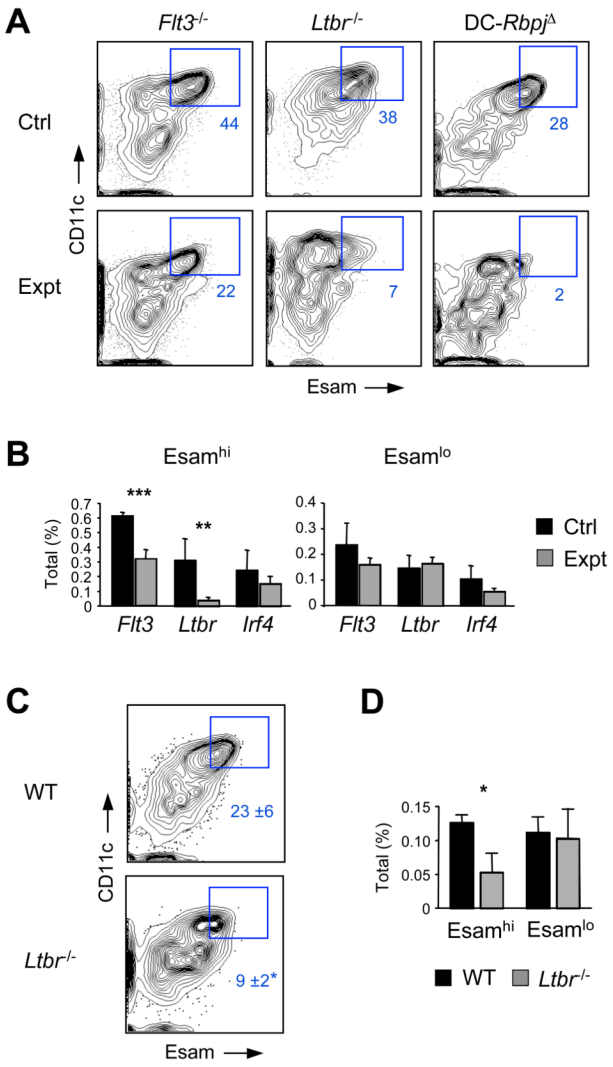

Figure 3. The development of Esam^{hi} CD11b^{+} cDCs requires LTβR signaling

(A) Splenic CD11b^{+} Esam^{hi} DC subset in experimental (Expt) *Flt3*$^{-/-}$ or *Ltbr*$^{-/-}$ animals or respective wild-type controls (Ctrl). The DC-*Rbpj*$^{\Delta}$ splenocytes that lack Esam^{hi} DCs (Fig. 2D) are included for comparison. Shown are staining profiles of gated B220^{-} CD11b^{+} CD8^{-} splenocytes, with the CD11c^{hi} Esam^{hi} DC population highlighted.

(B) The fraction of Esam^{hi} and Esam^{lo} DC subsets among total splenocytes from *Flt3*$^{-/-}$, *Ltbr*$^{-/-}$ or DC-*Irf4*$^{\Delta}$ experimental (Expt) animals or controls (Ctrl). Significance is indicated as in Fig. 1.

(C) Splenic CD11b^{+} Esam^{hi} DC population among gated wild-type competitor (WT) or *Ltbr*$^{-/-}$ donor populations in competitively reconstituted BM chimeras, shown as in panel A (mean ± S.D. of 3 animals).

(D) The fraction of WT competitor- or *Ltbr*$^{-/-}$ donor-derived CD11b^{+} DC subsets among total splenocytes in the BM chimeras (mean ± S.D. of 3 animals).

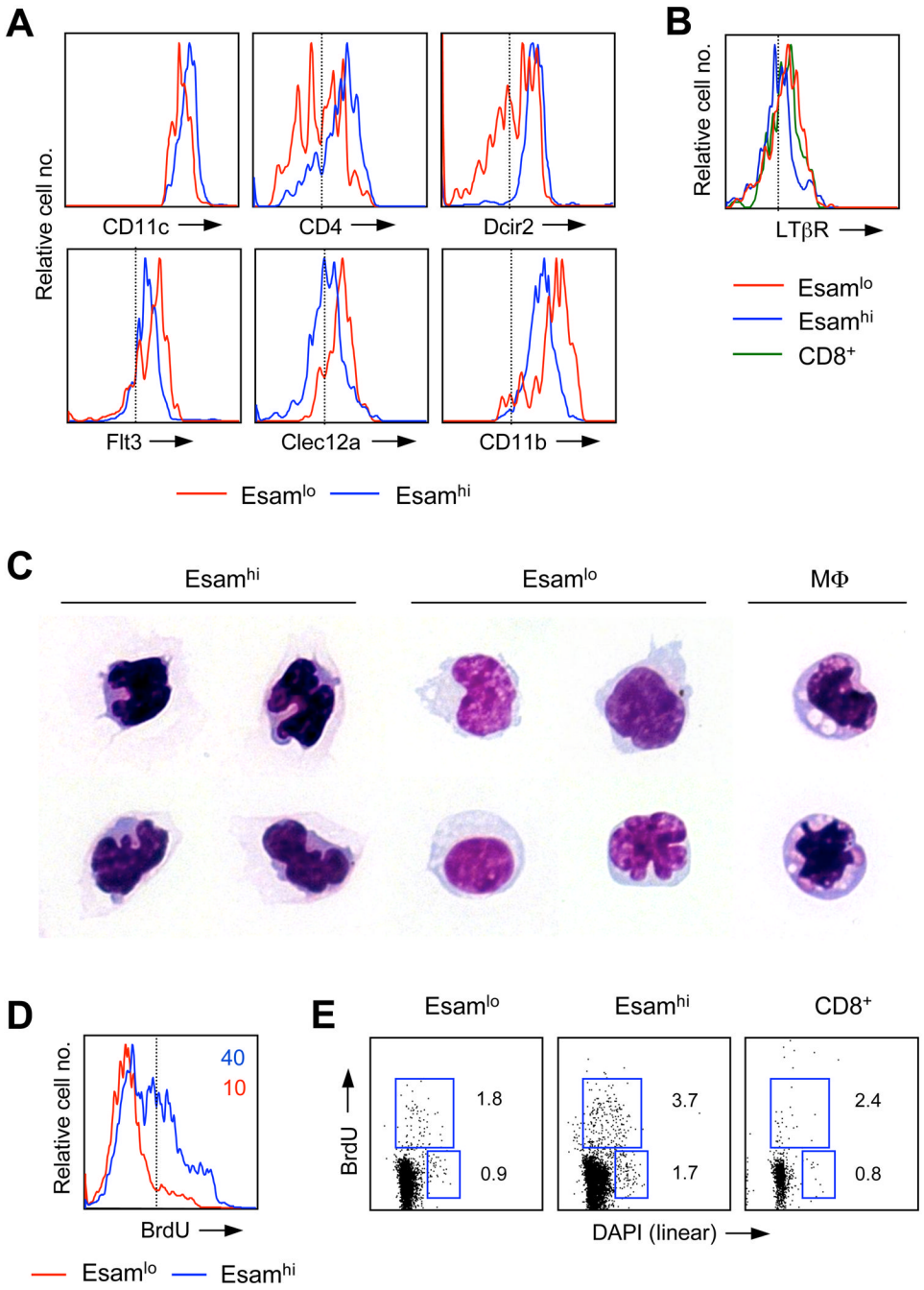

Figure 4. Phenotypic analysis of the splenic CD11b^{+} DC subsets

Unless indicated otherwise, *Cx3cr1*-GFP reporter mice were used to separate the Esam^{hi} GFP^{lo} and Esam^{lo} GFP^{hi} subsets of CD11c^{hi} CD11b^{+} CD8^{-} splenic DCs.

(A) Expression of the indicated surface markers in the gated Esam^{hi} GFP^{lo} and Esam^{lo} GFP^{hi} subsets. Dashed lines indicate positive staining threshold.

(B) Expression of LTβR on the indicated DC subsets from wild-type mice.

(C) Microphotographs of the sorted DC subsets stained by Giemsa stain on cytospin preparations. The CD11c^{-} CD11b^{+} F4/80^{+} *Cx3cr1*-GFP^{+} macrophages (MΦ) are shown for comparison (magnification, 400x).

(D) Histograms of BrdU staining in the gated DC subsets after 2 days of in vivo BrdU pulse. The percentages of $BrdU^+$ cells are indicated; representative of 4 animals.
(E) Cell cycle profiles of DC subsets after 2 hr of in vivo BrdU pulse. Shown are gated DC subsets stained for DNA content (DAPI) and BrdU incorporation; the fractions of cells in S and G2/M phases are indicated (representative of 2 animals).

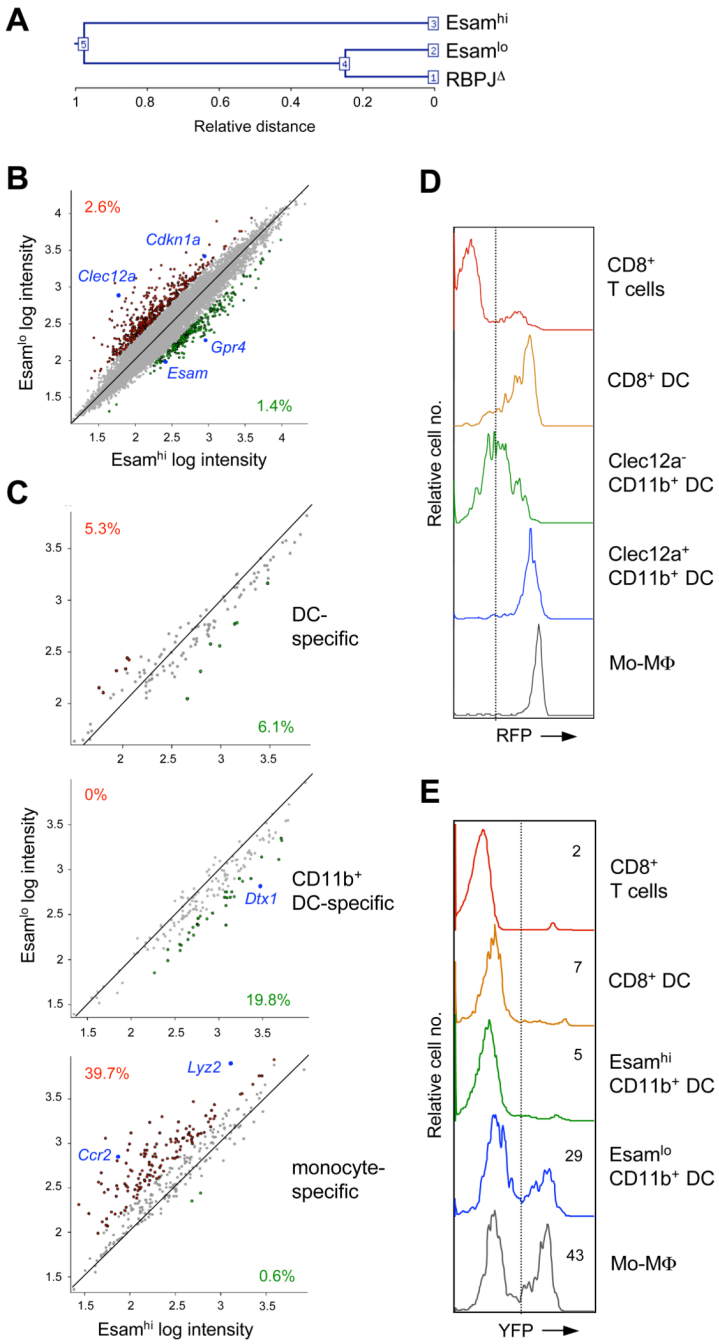

Figure 5. Gene expression profiles of splenic CD11b$^+$ DC subsets

(A) The comparison of control and RBPJ-deficient CD11b$^+$ DCs. Splenic CD11b$^+$ DCs from *Cx3cr1*-GFP$^+$ DC-*Rbpj*$^\Delta$ mice were sorted along with the Esam^{hi} GFP^{lo} and Esam^{lo} GFP^{hi} subsets of CD11b$^+$ splenic DCs from control *Cx3cr1*-GFP$^+$ mice. Shown is unsupervised clustering analysis of the resulting microarray expression profiles.

(B) Pairwise comparison of the Esam^{hi} and Esam^{lo} subsets. The probes overexpressed >2 fold in the respective populations are shown in green and red, and their percentage among the total probes is indicated. Probes for select relevant genes are highlighted in blue.

(C) The expression of signature probe sets in the Esam^{hi} and Esam^{lo} subsets. The signature sets of total DCs, CD11b^{+} DCs and monocytes were derived from Immgen database and their distribution among the Esam^{hi} and Esam^{lo} subsets is depicted as in panel B.
(D) The expression of *Ccr2*-RFP reporter in DC subsets. Shown are histograms of RFP expression in the indicated splenic populations including CD11c^{-} CD11b^{+} monocytes and macrophages (Mo-MΦ), and Clec12a^{-} and Clec12a^{+} CD11b^{+} DCs corresponding to Esam^{hi} and Esam^{lo} subsets, respectively.
(E) Efficiency of *Lyz2-cre* recombination in DC subsets. Shown are histograms of YFP expression in the indicated splenic populations of *Lyz2-cre*$^{+}$ mice with *cre*-inducible YFP reporter allele.

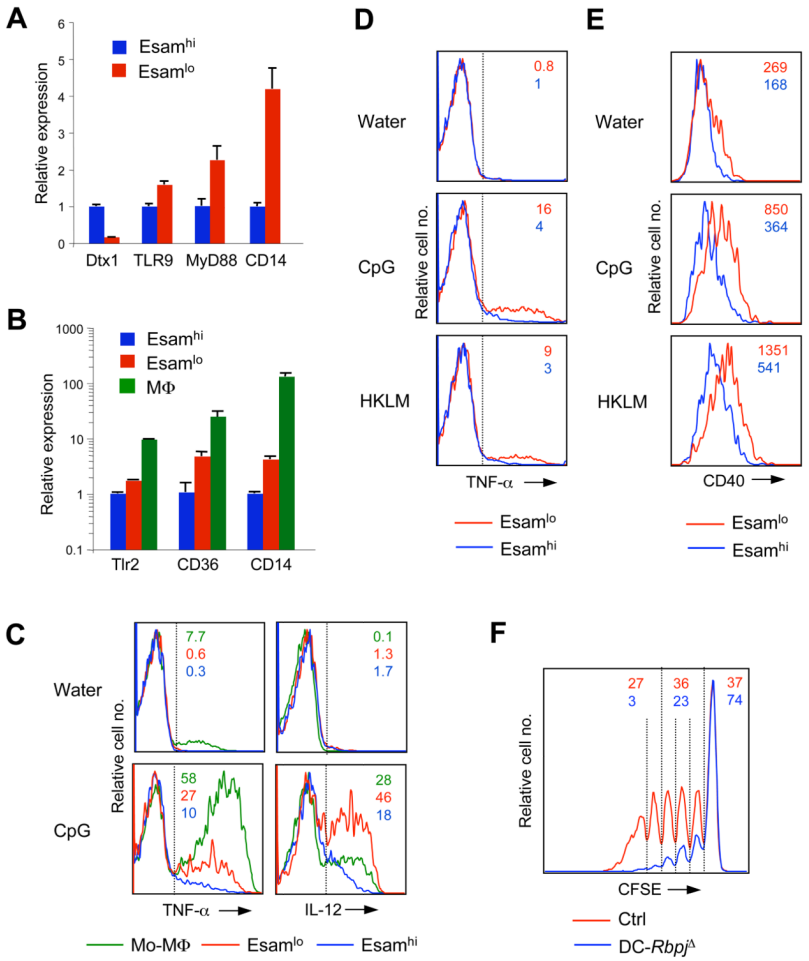

Figure 6. Functional properties of splenic CD11b$^+$ DC subsets

(A) The expression of indicated genes in GFP^{lo} Esam^{hi} and GFP^{hi} Esam^{lo} subsets of splenic CD11b$^+$ DCs sorted from *Cx3cr1*-GFP mice. Data represent normalized expression values relative to the Esam^{hi} sample as determined by qPCR (mean ± S.D. of triplicate reactions).

(B) The expression of indicated genes in the same DC subsets as well as in CD11c$^-$ CD11b$^+$ F4/80$^+$ GFP$^+$ macrophages (MΦ), determined by qPCR as in (A) and shown on a log scale.

(C) Cytokine production by CD11b$^+$ DCs in response to TLR9 ligand CpG. Lymphocyte-depleted splenocytes from *Cx3cr1*-GFP mice were incubated for 6 hr with CpG and stained for surface markers and intracellular TNF-α or IL-12. Shown are cytokine expression profiles in GFP^{lo} Esam^{hi} or GFP^{hi} Esam^{lo} subsets of CD11c^{hi} CD11b$^+$ DCs, or in CD11c$^-$ CD11b$^+$ GFP^{hi} monocytes and macrophages (Mo-MΦ). Data are representative of three independent experiments.

(D) TNF-α production by CD11b$^+$ DCs in response to TLR ligands. Splenocytes from *Cx3cr1*-GFP mice were activated with CpG or TLR2 ligand heat-killed *L.monocytogenes* (HKLM) and stained as above.

(E) Phenotypic maturation of CD11b$^+$ DCs in vitro. Splenocytes from *Cx3cr1*-GFP mice were activated with CpG or HKLM and stained for DC markers as above. Shown are staining profiles of CD11b$^+$ DC subsets for CD40, with mean fluorescence intensities indicated.

(F) In vivo CD4$^+$ T cell priming in the absence of Esam^{hi} DCs. DC-*Rbpj*^{Δ} or littermate control (Ctrl) mice were administered CFSE-labeled OVA-specific OT-II T cells and immunized with OVA. Shown are CFSE staining profiles of gated OT-II T cells from the

recipient spleens 3 days after immunization. The fractions of T cells that did not divide or divided 1–3 and >3 times are indicated (mean of two recipients).

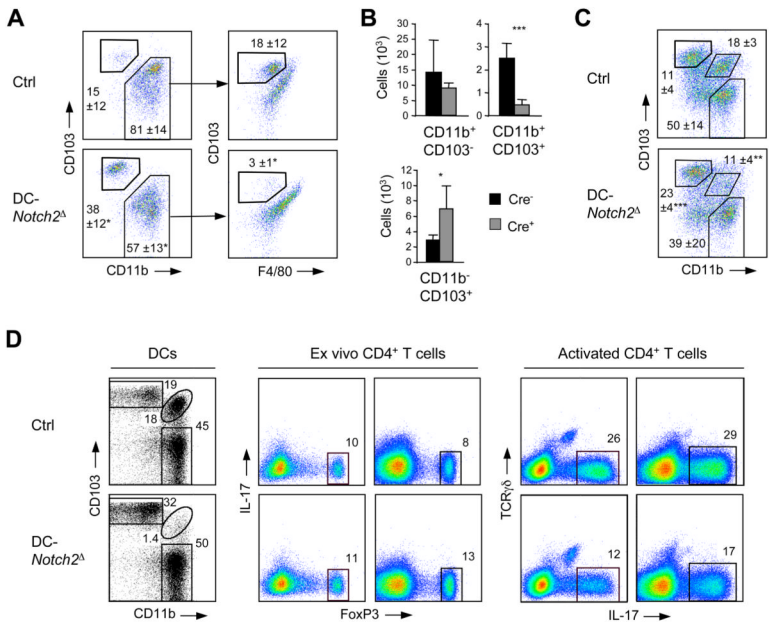

Figure 7. Notch2 controls the development of intestinal CD11b^{+} CD103^{+} DCs

(A) DC populations in the intestinal lamina propria from DC-*Notch2*$^{\Delta}$ mice and littermate controls. Shown are staining profiles of CD45^{+} CD11c^{hi} MHC II^{+} DCs and of the gated CD11b^{+} DCs, highlighting the CD11b^{+} CD103^{+} DC subset. Fractions represent average ± S.D. of 4 animals per group. Statistical significance is indicated as in Fig. 1.

(B) Absolute numbers of the indicated DC subsets (mean ± S.D. of 4 animals).

(C) Staining profiles of CD11c^{hi} MHC II^{+} DCs from the mesenteric lymph nodes. Fractions represent average ± S.D. of 7 animals per group.

(D) Effector T cell populations in the intestine. Lymphocytes were isolated from the LP of small intestine and stained ex vivo for intracellular FoxP3 or activated in vitro with PMA plus ionomycin and stained for intracellular IL-17. Shown are profiles of CD11c^{hi} MHC II^{+} LP DCs and of gated TCRβ^{+} CD4^{+} T cells isolated ex vivo or activated in vitro (two pairs of littermates shown; representative of 4 DC-*Notch2*$^{\Delta}$ animals).